



## Regular article

## Divergent strain acceleration effects in metallic glasses

Z. Lu<sup>a</sup>, X.N. Yang<sup>b</sup>, B.A. Sun<sup>c</sup>, Y.Z. Li<sup>a</sup>, K. Chen<sup>b</sup>, W.H. Wang<sup>a</sup>, H.Y. Bai<sup>a,\*</sup><sup>a</sup> Institutes of Physics, Chinese Academy of Sciences, Beijing 100190, China<sup>b</sup> Beijing National Laboratory for Condensed Matter Physics and Key Laboratory of Soft Matter Physics, Institute of Physics, Chinese Academy of Sciences, Beijing 100190, China<sup>c</sup> Center for Advanced Structural Materials, Department of Mechanical and Biomedical Engineering, City University of Hong Kong, Hong Kong

## ARTICLE INFO

## Article history:

Received 11 November 2016

Received in revised form 10 December 2016

Accepted 12 December 2016

Available online xxxx

## Keywords:

Bulk metallic glass

Relaxation

Anelastic behavior

Strain rate sensitivity

Temperature-strain equivalence

## ABSTRACT

Relaxation is a key feature in glassy physics, and the strain-induced effects on relaxations in metallic glasses are of practical significance, yet still unclear. Through a contrastive combination of dynamical mechanical spectroscopy and linear-heating stress relaxation methods, we find that strain effectively facilitates the relaxation dynamics with divergent modulation behaviors in a wide temperature range for metallic glasses. Two loading modes are coupled with linear-heating, and we experimentally confirm the “temperature-strain equivalence”. Our results benefit for better understanding the unique effect of strain on relaxation and for providing guidance on applications of metallic glasses with improved performances at different temperatures.

© 2016 Published by Elsevier Ltd on behalf of Acta Materialia Inc.

During glass transition, atoms are trapped into glassy states, which are in various potential energy valleys [1–5]. While glassy materials behave like solids as a whole below the glass transition temperature  $T_g$ , thermal energy could activate local atomic motions or locally unjammed atoms, by which relaxations occur. These atoms constitute flow units, accommodate the flow and lead to deformation behaviors in glasses [6–9]. When the cluster density of flow units reaches a critical value, the percolation of flow units occurs and the entire glass system can unjam from a frozen state into a supercooled liquid state [3,9–11]. The flow units can also be activated by external strain [12,13], which plays an equivalent role as temperature in the systems such as granular materials and foams. In thermal systems including colloidal and metallic glasses (MGs), both thermal and mechanical stimulations can lead to unjamming. Although the interplay among thermal energy, applied force, and packing constraint has been intensely studied in colloidal systems [14–16], there is few investigation into the interaction between temperature and strain in the jamming theory for MGs. This investigation would be of practical importance because MGs, serving as structural materials with unique mechanical property, suffer from complex mechanical and thermal circumstances. Clarifying the effect of strain under different loading modes and thermal invigoration on relaxations would also contribute to understanding the behavior of shear bands [12, 17–19], plastic deformation, and fracture morphology patterns [20,21]. Recently, the strain effects such as strain-induced glass transition and mechanical flow have been investigated by molecular dynamics

simulations [7,14,22]. The elastostatic compression strain applied on MGs can create irreversible structural disordering and cause permanent deformation at room temperature [23,24]. However, experimentally, the effect of strain on relaxation under different loading modes at different temperatures, the direct examination of ‘strain-temperature equivalence’ and the jamming phase diagram for MGs are still unclear.

In this Letter, we use dynamical mechanical spectroscopy (DMS, a dynamical loading mode) and linear-heating stress relaxation (a quasi-static loading mode) methods to study the effect of external loading on MG relaxations in a wide temperature range. We find that strain effectively facilitates the occurrence of  $\alpha$ -relaxation (glass transition) but has negligible effect on  $\beta$ -relaxation (low temperature relaxation) in the dynamic loading mode, while in the quasi-static loading mode the strain has significant impact on low temperature relaxation. The concept of ‘strain-temperature equivalence’ and the jamming diagrams with different loading modes of MGs are constructed to understand the impact of strain on the jamming-unjamming transition of MGs system at different temperatures.

A typical  $\text{La}_{55}\text{Ni}_{20}\text{Al}_{25}$  (in atomic percent) MG was selected for experiments for its pronounced  $\beta$ -relaxation behavior. The MG ribbon with the thickness of 30  $\mu\text{m}$  was prepared using a melt-spinning technique and the glassy nature of the sample was ascertained by X-ray diffraction and differential scanning calorimeter. Two different loading modes were applied to the MG ribbons. The dynamical loading was performed with a TA Q800 dynamical mechanical analyzer (DMA) by uniaxial tension method with a heating rate of 3 K/min, testing frequency  $f = 1$  Hz with varied strain amplitudes. The other deformation mode is a constant loading mode performed through the same DMA with various tension strains at the same linear heating rate of 3 K/min [25].

\* Corresponding author at: Institute of Physics, P.O. Box 603, Beijing 100190, China.  
E-mail address: [hybai@iphy.ac.cn](mailto:hybai@iphy.ac.cn) (H.Y. Bai).

The mechanical relaxation spectra of  $\text{La}_{55}\text{Ni}_{20}\text{Al}_{25}$  MG with different strains under dynamical loading are shown in Fig. 1(a). Regardless of strain amplitudes, the temperature dependence of loss modulus yields two distinct peaks. The peak in the range from 330 K to 420 K represents  $\beta$ -relaxation and the peak at a higher temperature corresponds to  $\alpha$ -relaxation. The emergence of  $\beta$ -relaxation peak indicates that a fraction of atoms locally are unjammed from frozen state and transform into flow units [26]. When the cluster density of flow units reaches a critical point, the percolation of flow units leads to the MG entirely unjamming and contributes to distinct  $\alpha$ -relaxation (or occurrence of glass transition) [27] as shown in Fig. 1(a). In order to investigate the strain modulation of relaxation under dynamic loading, a series of strain amplitudes were applied to the glass ribbons. The  $\beta$ -relaxation peak remains almost unchanged with strain increased from 0.07% to 0.4%, while the  $\alpha$ -relaxation peak shifts to low temperatures with sharply decreased intensity. To quantitatively certify the invariable of  $\beta$ -relaxation, the Arrhenius equations are used to fit the  $\beta$  relaxation process and the fitting results are presented in the Supplemental Data and Fig. S1 and Table S1. The inset of Fig. 1(a) shows the strain amplitude dependences of the intensity and peak temperature for the  $\alpha$ -relaxation.

Our previous work shows that the MGs can be considered as a fraction of separated flow units confined in an elastic matrix [9,28] as shown in Fig. 1(b). We quantitatively rationalize the distinguished strain modulation effects on  $\alpha$ - and  $\beta$ -relaxations under the dynamical

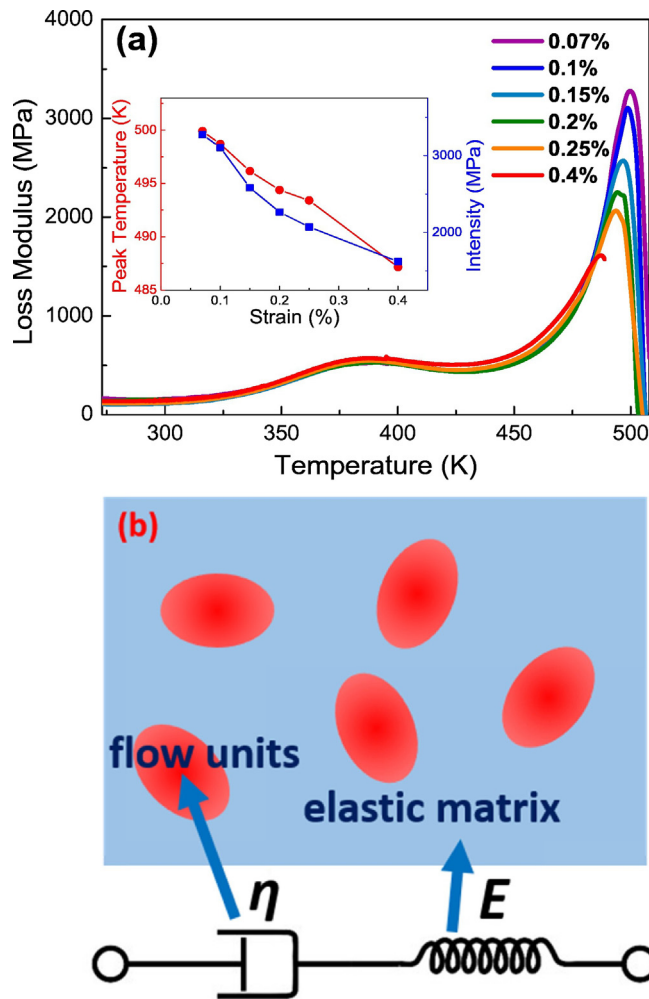


**Fig. 1.** (a) The loss modulus  $G''$  as a function of temperature for different strain amplitudes. The inset shows the relation between strain amplitude, peak temperature and intensity of  $\alpha$ -relaxation. (b) The schematic illustration of Maxwell model and flow units model: the flow units are surrounded by elastic matrix and present viscosity behavior.

loading using Maxwell model [29], in which flow unit is represented by a dashpot and the elastic glassy matrix by spring. The total strain  $\varepsilon$  can be written as:

$$\frac{d\varepsilon}{dt} = \frac{\sigma}{\eta} + \frac{1}{E} \frac{d\sigma}{dt}, \quad (1)$$

where  $\sigma$  is the stress,  $\eta$  is the viscosity of flow units and  $E$  is Young's modulus of the matrix. In DMA, the applied sinusoidal strain is  $\varepsilon = \varepsilon_0 \exp(i\omega t)$ , and the resulting stress is  $\sigma = \sigma_0 \exp(i\omega t + \delta)$ , where  $\omega$  is the applied frequency and  $\delta$  is the phase difference between stress and strain. Eq. (1) can be rewritten as  $i\omega\varepsilon = \sigma/\eta + i\omega\sigma/E$  and the loss modulus is [30]:

$$G''(\omega) = \frac{\omega/\eta}{(1/\eta)^2 + (\omega/E)^2} = \frac{\omega\alpha\Omega}{k_B T} \exp\left(-\frac{W}{k_B T}\right) / \left\{ \left[ \frac{\alpha\Omega}{k_B T} \exp\left(-\frac{W}{k_B T}\right) \right]^2 + (\omega/E)^2 \right\}, \quad (2)$$

where  $\alpha$  is the material's characteristic strain rate,  $k_B$  is the Boltzmann constant,  $W$  and  $\Omega$  are the energy barrier and volume for flow units, respectively. When the temperature  $T = T_g$ , the energy barrier for  $\alpha$ -relaxation can be expressed as [31]  $W_{\tau,\alpha} = \beta T_g [(\tau_c - \tau)/\tau_c]^{3/2}$ , where  $\beta$  is constant,  $\tau$  is shear stress and  $\tau_c$  is critical yield stress. Thus, Eq. (2) can be rewritten as:

$$G''(\omega) = \frac{\omega C f(\tau)}{[C f(\tau)]^2 + (\omega/E)^2}, \quad (3)$$

where  $C = \alpha\Omega/k_B T_g$  is constant by assuming that the flow units of  $\text{La}_{55}\text{Ni}_{20}\text{Al}_{25}$  MG have the same constant volume, and  $f(\tau) = \exp[-\beta/k_B(1 - \tau/\tau_c)^{3/2}]$ . For DMS experiments,  $W_{\tau,\alpha}$  can be effectively decreased by increasing the applied strain, and thus the flow units can be activated at relatively lower temperatures [32] and the temperature of  $\alpha$ -relaxation peak moves toward low temperatures as shown in Fig. 1(a). Meanwhile,  $G''(\omega)$  has a significant inverse relation with  $f(\tau)$  according to Eq. (3), and the value of  $f(\tau)$  will increase with the enhanced strain or stress. Therefore, strain or stress can reduce the intensity of  $\alpha$ -relaxation peak, and our theoretical analysis is consistent with the experiment observation that the intensity of  $\alpha$ -relaxation peak is weakened by incremental strain [see Fig. 1(a)]. However, when the temperature is much lower than  $T_g$ , the  $\alpha$ -relaxation is suppressed. The energy barrier of  $\beta$ -relaxation can be expressed as [18]:  $W_{\tau,\beta} = 4R G_{0T} \gamma^2 C (1 - \tau/\tau_c)^{3/2} \zeta \Omega$ , where  $R = \pi^2/32$ ,  $\gamma_c = 0.027$ ,  $\zeta = 3$ , the shear modulus  $G_{0T} = 19.4$  GPa, and the volume of flow units is about  $5.31 \text{ nm}^3$  for  $\text{La}_{55}\text{Ni}_{20}\text{Al}_{25}$  [33]. For the DMS experiments,  $\tau/\tau_c$  varies from 0.035 to 0.2 (strain changes from 0.07% to 0.4% in the apparent elastic regime ~2% of the MG), and the energy barrier  $W_{\tau,\beta}$  varies from 1.64 eV down to 1.24 eV. However, the thermal activation energy  $E_T = 0.937$  eV at the peak temperature for  $\beta$ -relaxation of 380 K for linear heating process, and the mechanical energy  $E_S = \gamma\tau\Omega$  changes from 0.046 eV to 0.26 eV as strain varies from 0.07% to 0.4%, where  $\gamma = 0.1$  is shear strain of flow units [30]. Even though applied strain can decrease energy barrier, the combined thermal and mechanical activation energy are still well below the value of energy barrier for the  $\beta$ -relaxation of the MG, thus the increased strain cannot activate more flow units, which causes the intensity and temperature of  $\beta$ -relaxation peak remain nearly unchanged as shown in Fig. 1(a).

Glass is in non-equilibrium state and its relaxation behaviors are time dependent [34]. Aside from the modulation of relaxation under dynamical loading, we also investigate the stress relaxation under constant strain with the same heating rate. Fig. 2(a) shows the stress relaxation upon heating with various strains for  $\text{La}_{55}\text{Ni}_{20}\text{Al}_{25}$ , the stress is normalized by initial stress  $\sigma_0$ . Under the strain of 0.4%, the stress of the sample starts to drop at about 350 K. As the strain increases, the obvious stress relaxation tends to occur at lower temperatures. This

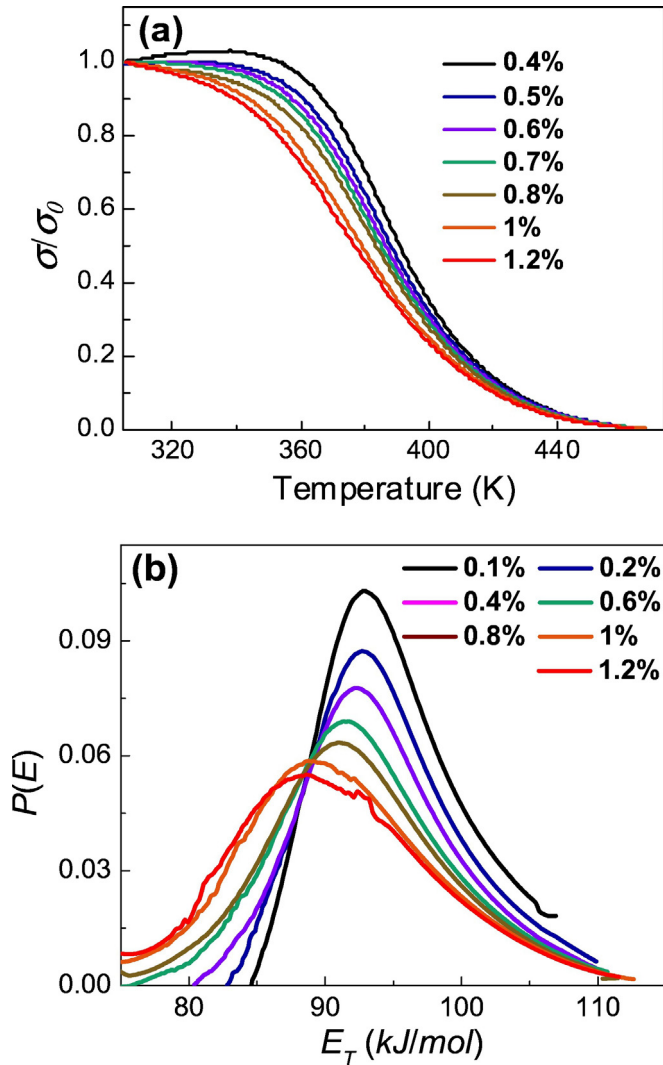


**Fig. 2.** (a) The tension stress relaxation curves under linear heating with various strains for  $\text{La}_{55}\text{Ni}_{20}\text{Al}_{25}$ , the stress is normalized by initial stress  $\sigma_0$ . (b) The activation energy spectra of  $\text{La}_{55}\text{Ni}_{20}\text{Al}_{25}$  for different strains.

tendency suggests that static strain accelerates the relaxation dynamics of the MG samples.

Using the activation energy spectrum model [35], we obtained the activated energy distribution of unjammed flow units in MG for various strains as shown in Fig. 2(b), where  $P(E)$  is the total available property change induced by all the activation processes. The activation energy spectra of flow units present a broad distribution, suggesting that the mechanical and dynamical behaviors of glass forming system are heterogeneous [36–38]. With applied strain increasing from 0.1% to 1.2%, the activation energy spectra shift toward to lower values with a wider full width at half maximum (FWHM). This strain dependence of activation energy spectra suggests that a larger strain can activate more flow units at a relatively lower temperature and the strain acceleration effect is similar to those in other glass-forming systems [39,40].

The previous work shows that both strain and temperature can accelerate relaxation dynamics and a sufficient strain could lead to jamming-unjamming transition [14,41]. However, the ‘strain-temperature equivalence’ relation is obtained only in granular, colloidal experiments or simulated systems [7,35]. We extend these concepts into metallic glassy systems in quasi-static relaxation mode. The internal stresses that originates from the quenching process are released at the initial relaxation procedure and the strain acceleration effect can be almost ignored at high temperatures as shown in Fig. 4(b). Based on the above

analysis, we focus on the low temperature regime where stress relaxation is readily influenced by strain amplitude, and extract the relation between stress relaxation and thermal energy as shown in Fig. 3(a). The stress from the unjamming process shows a monotonic decrease with increasing thermal energy. For a larger strain of  $\varepsilon = 1.2\%$ , the stress in MG relaxes more rapidly at the same applied thermal energy. Alternatively, the MG with higher applied strain can realize the same relaxation degree at relatively lower thermal energies or temperatures. As both strain and temperature can facilitate the relaxation process, we define an effective energy  $E = E_T + cE_S$ , where  $E_T$  is the contribution from thermal energy,  $c$  represents the degree of contribution from mechanical energy  $E_S$ . Based on this effective energy, the stress relaxation curves with different strains collapse into a universal decay as shown in Fig. 3(b) (The total relaxation curves are presented in the Supplemental Data and Fig. S2). This universality indicates that strain plays a similar role in stress relaxation as temperature does. For example, as shown in Fig. 3(b), an applied energy of 0.892 eV realizes residual stress  $\sigma/\sigma_0 = 0.8$  and this energy can be provided through different combinations of temperature or strain. The monotonic strain dependence of parameter  $c$  in the inset of Fig. 3(b) suggests that mechanical energy  $E_S$  plays more and more important role with increasing strain.

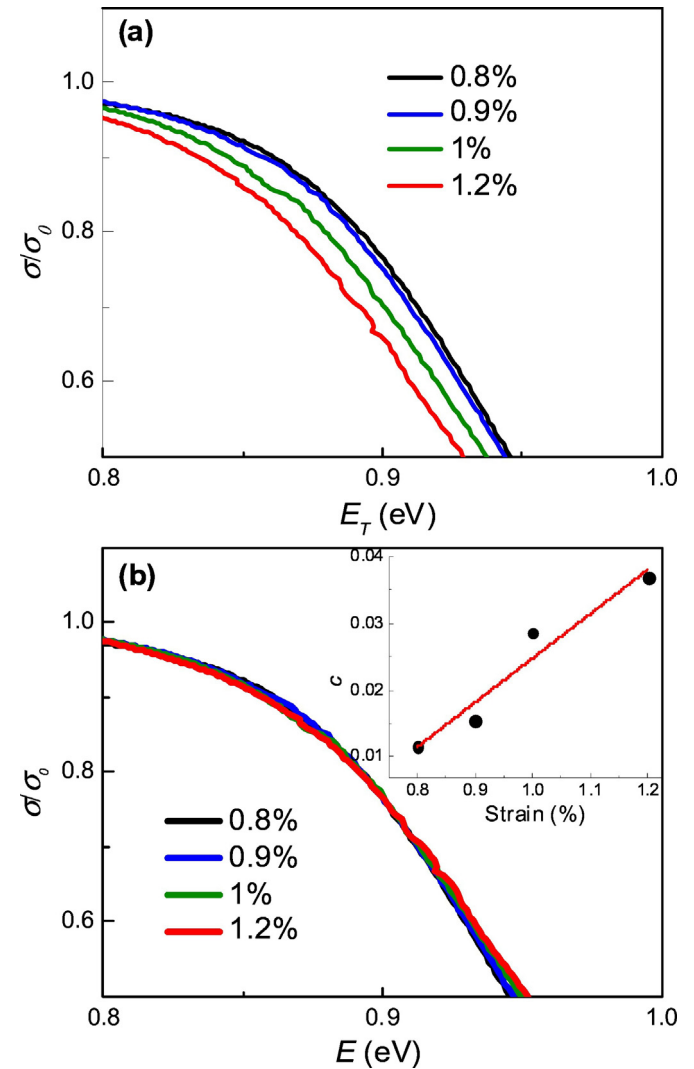


**Fig. 3.** (a) The relation between stress relaxation and thermal activation energy. (b) Combination of the strain effect and definition effective energy  $E$ , the stress relaxation curves for different strains can overlap together. The inset shows the tendency of parameter  $c$  with increasing strain.

The above experimental results show that the strain speeds up the relaxation dynamics and exhibits different effects under two different loading modes. The phase diagrams for jamming in MGs can thus be constructed based on strain and temperature as shown in Fig. 4(a) and (b). The white round dots in Fig. 4(a) are the  $\alpha$  relaxation peak temperatures or the jamming transition temperature for various strains, and the yellow curves denote the boundary between jammed phase and unjammed phase. It can be seen that increasing of strain leads to decreasing of transition temperature. However, the low temperature relaxation mode ( $\beta$  relaxation) is not under the control of strain acceleration effect as shown in Fig. 1(a). At relatively lower temperature, even though the applied strain is increased, the total applied energy (thermal and mechanical energy) is still below the activation energy of flow units, the increased strain has little effect on the unjamming behavior of metallic glass. This diagram quantitatively demonstrates how strain amplitude accelerates  $\alpha$  relaxation in the dynamical loading mode. Fig. 4(b) recasts the same data of Fig. 2(a) in contour plots as a two-dimensional function of strain and temperature, and the white curves are the iso-stress lines. At low temperature region (especially below 380 K), the iso-stress line leans to the low temperature side

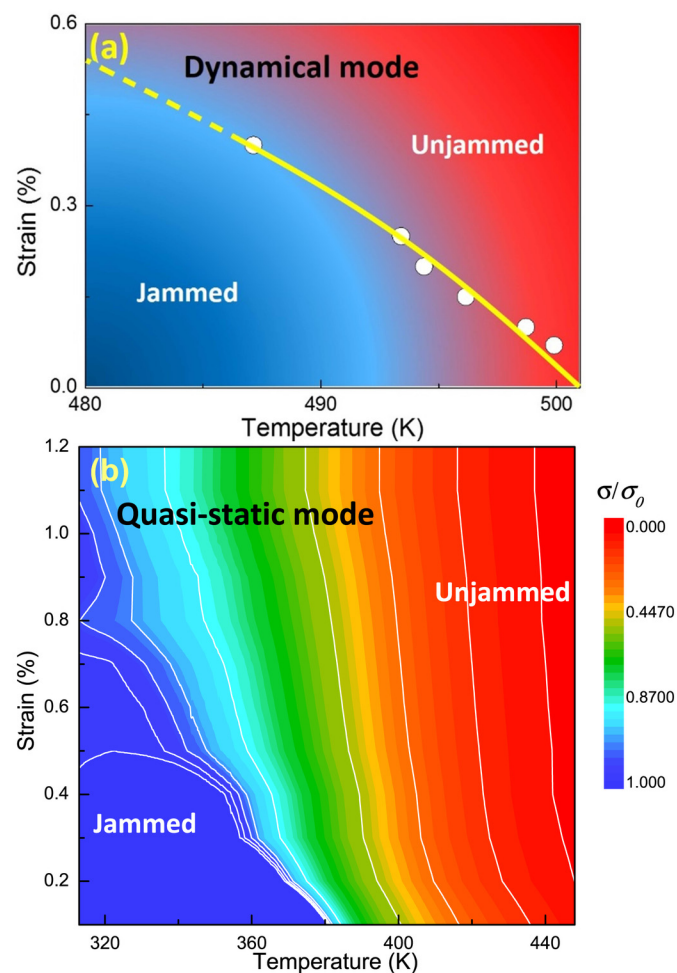


**Fig. 4.** An experimental jamming phase diagram of dynamical mode (a) and quasi-static mode (b) for MGs. (a) The white round dots present the  $\alpha$  relaxation peak temperatures for various strains, and the yellow dashed curve shows the changing trend of the  $\alpha$  relaxation peak temperature with strain. The yellow dashed and solid curves denote the boundary between jammed phase and unjammed phase. In dynamic mode, strain accelerates the high temperature jamming process. (b) Two-dimensional plot of stress as a function of temperature and strain and the white curves are iso-stress lines. Note that the iso-stress line leans to the low temperature side with the increasing strain. The strain presents different effects for unjamming process in different relaxation modes. (For interpretation of the references to color in this figure legend, the reader is referred to the web version of this article.)

with the incremental strain. This strong dependence of strain suggests that strain effectively accelerates the stress relaxation at a relatively low temperature. With increasing temperature, the gradient of iso-stress lines increase. At 440 K, the iso-stress line is nearly vertical and thus only weakly dependent on strain amplitude, which suggests that at high temperatures the strain-acceleration effect can be ignored, and the stress relaxation is solely determined by the temperature.

In dynamical mode, strain effectively accelerates the high temperature unjamming process and has negligible effect on low temperature relaxation process, which is in contrast to the quasi-static mode. Our results suggest that the strain-induced unjamming and relaxation processes in MGs are temperature and loading modes dependent. MGs have diverse and unique mechanical properties with great application potentials, but the suitable working environment is still unclear. The above comparative experiments have the benefits of providing guidance to the application of MGs. For example, in practical applications, MGs can maintain well performance over a wide temperature range for dynamical mechanical conditions and should avoid static working environment.

In summary, we demonstrate that strain can make the flow units unjam from frozen state and accelerate the process of glass transition. We show that the concept of 'strain-temperature equivalence' can be extended into MG system, and construct jamming phase diagrams for MG under different loading modes. The results provide macroscopic insights to the mechanism of strain-effect in MGs and can also guide the practical application of MGs.

## Acknowledgements

Experimental assistance with PF Guan, DQ Zhao, MX Pan, YT Sun and C Wang is appreciated. This work was supported by the NSFC (51271195) and MOST 973 Program (2015CB856800).

## Appendix A. Supplementary data

Supplementary data to this article can be found online at <http://dx.doi.org/10.1016/j.scriptamat.2016.12.017>.

## References

- [1] J.C. Dyre, *Rev. Mod. Phys.* 78 (2006) 953–972.
- [2] P.G. Debenedetti, F.H. Stillinger, *Nature* 410 (2001) 259–267.
- [3] A.J. Liu, S.R. Nagel, *Nature* 396 (1998) 21–22.
- [4] H.N. Lee, K. Paeng, S.F. Swallen, M.D. Ediger, *Science* 323 (2009) 231–234.
- [5] P. Olsson, S. Teitel, *Phys. Rev. Lett.* 99 (2007) 178001.
- [6] J.S. Langer, *Phys. Rev. E* 78 (2008) 051115.
- [7] P.F. Guan, M.W. Chen, T. Egami, *Phys. Rev. Lett.* 104 (2010) 205701.
- [8] W.H. Wang, Y. Yang, T.G. Nieh, C.T. Liu, *Intermetallics* 67 (2015) 81–86.
- [9] Z. Lu, W. Jiao, W.H. Wang, H.Y. Bai, *Phys. Rev. Lett.* 113 (2014) 045501.
- [10] F. Faupel, W. Frank, M.P. Macht, H. Mehrer, V. Naundorf, K. Rätzke, H.R. Schober, S.K. Sharma, H. Teichler, *Rev. Mod. Phys.* 75 (2003) 237–280.
- [11] D.Z. Chen, C.Y. Shi, Q. An, Q. Zeng, W.L. Mao, W.A. Goddard, J.R. Greer, *Science* 349 (2015) 1306–1310.
- [12] J.J. Lewandowski, A.L. Greer, *Nat. Mater.* 5 (2006) 15–18.
- [13] M.L. Falk, J.S. Langer, *Annu. Rev. Condens. Matter Phys.* 2 (2011) 353–373.
- [14] H.B. Yu, R. Richert, R. Maaß, K. Samwer, *Nat. Commun.* 6 (2015) 7179.
- [15] N.C. Keim, P.E. Arratia, *Soft Matter* 9 (2013) 6222–6225.
- [16] Z. Zhang, N. Xu, D.T.N. Chen, P. Yunker, A.M. Alsayed, K.B. Aptowicz, P. Hbadas, A.J. Liu, S.R. Nagel, A.G. Yodh, *Nature* 459 (2009) 230–233.
- [17] R. Dasgupta, H.G.E. Hentschel, I. Procaccia, *Phys. Rev. Lett.* 109 (2012) 255502.
- [18] M.D. Demetriou, J.S. Harmon, M. Tao, G. Duan, K. Samwer, W.L. Johnson, *Phys. Rev. Lett.* 97 (2006) 065502.
- [19] Y.H. Liu, C.T. Liu, W.H. Wang, A. Inoue, T. Sakurai, M.W. Chen, *Phys. Rev. Lett.* 103 (2009) 065504.
- [20] C.C. Hays, C.P. Kim, W.L. Johnson, *Phys. Rev. Lett.* 84 (2000) 2901.
- [21] G. Wang, D.Q. Zhao, H.Y. Bai, M.X. Pan, A.L. Xia, B.S. Han, X.K. Xi, Y. Wu, W.H. Wang, *Phys. Rev. Lett.* 98 (2007) 235501.
- [22] H.B. Yu, R. Richert, R. Maaß, K. Samwer, *Phys. Rev. Lett.* 115 (2015) 135701.
- [23] K.W. Park, C.M. Lee, M.R. Lee, E. Fleury, M.L. Falk, J.C. Lee, *Appl. Phys. Lett.* 94 (2009) 021907.
- [24] K.W. Park, C.M. Lee, M. Wakeda, Y. Shitubani, M.L. Falk, J.C. Lee, *Acta Mater.* 56 (2008) 5440–5450.
- [25] V.A. Khonik, A.T. Kosilov, *J. Non-Cryst. Solids* 170 (1994) 270–277.

- [26] H.B. Yu, X. Shen, Z. Wang, L. Gu, W.H. Wang, H.Y. Bai, *Phys. Rev. Lett.* 108 (2012) 015504.
- [27] K.L. Ngai, Z. Wang, X.Q. Gao, H.B. Yu, W.H. Wang, *J. Chem. Phys.* 13 (2013) 014502.
- [28] Z. Wang, P. Wen, L.S. Huo, H.Y. Bai, W.H. Wang, *Appl. Phys. Lett.* 101 (2012) 121906.
- [29] J.D. Ferry, *Viscoelastic Properties of Polymers*, Wiley, New York, 1961.
- [30] A.S. Argon, *Acta Metall.* 27 (1979) 47–58.
- [31] W.L. Johnson, K. Samwer, *Phys. Rev. Lett.* 95 (2005) 195501.
- [32] D.J. Lacks, M.J. Osborne, *Phys. Rev. Lett.* 93 (2004) 255501.
- [33] S.T. Liu, Z. Wang, H.L. Peng, H.B. Yu, W.H. Wang, *Scr. Mater.* 67 (2012) 9–12.
- [34] J.C. Dyre, T. Christensen, N.B. Olsen, *J. Non-Cryst. Solids* 352 (2006) 4635–4642.
- [35] M.R.J. Gibbs, J.E. Evetts, J.A. Leake, *J. Mater. Sci.* 18 (1983) 278–288.
- [36] T. Fujita, K. Konno, W. Zhang, V. Kumar, M. Matsuura, A. Inoue, T. Sakurai, M.W. Chen, *Phys. Rev. Lett.* 103 (2009) 075502.
- [37] Y.H. Liu, D. Wang, K. Nakajima, W. Zhang, A. Hirata, T. Nishi, A. Inoue, M.W. Chen, *Phys. Rev. Lett.* 106 (2011) 125504.
- [38] P.Y. Huang, S. Kurasch, J.S. Alden, A. Shekhawat, A.A. Alemi, P.L. McEuen, J.P. Sethna, U. Kaiser, D.A. Muller, *Science* 342 (2013) 224–227.
- [39] V. Trappe, V. Prasad, L. Cipelletti, P.N. Segre, D.A. Weitz, *Nature* 411 (2001) 772–775.
- [40] M.E. Cates, J.P. Wittmer, J.P. Bouchaud, P. Claudin, *Phys. Rev. Lett.* 81 (1998) 1841–1844.
- [41] M.D. Ediger, C.A. Angell, S.R. Nagel, *J. Phys. Chem.* 100 (1996) 13200–13212.